

IMPLICATIONS OF THE PRONAOS OBSERVATIONS FOR THE LARGE SCALE SURVEYS WITH FIRST

J.-P. Bernard¹, A. Abergel¹, F. Boulanger¹, X. Dupac², M. Giard², G. Lagache¹, J.-M. Lamarre¹,
C. Meny², I. Ristorcelli², and B. Stepnik^{1,2}

¹Institut d'Astrophysique Spatiale (IAS), Bât. 121, Université Paris XI, F-91405 Orsay, France

²Centre d'Etude Spatial des Rayonnements (CESR), 9 av. Colonel Roche, BP 4346, F-31028 Toulouse, France

ABSTRACT

We present recent sub-millimeter (200-600 μm) observations obtained with the balloon experiment Pronaos. These have led to exciting and sometimes unexpected new results regarding the nature, the composition and chemistry of dust grains in the ISM. In particular, they reveal dust significantly colder than expected ($T=12\text{ K}$) in translucent and optically thin clouds at high galactic latitude, which can be interpreted as evidence for the existence of porous dust aggregates in diffuse clouds. The Pronaos observations also show a significant anticorrelation between dust equilibrium temperature and the spectral index of its emissivity law in the sub-millimeter. This may reflect quantum processes within the grains that appear only at low temperature and thus brings new insight on the nature of large dust grains in the ISM. Owing to the wavelength range covered and the high sensitivity achieved, the Pronaos observations prefigure what will be possible on large scale and higher angular resolution with FIRST. These results strongly argue in favor of a large survey of the diffuse ISM with FIRST and have direct implications about how to conduct such a survey.

Key words: ISM: dust property, continuum emission – Missions: PRONAOS, FIRST – Object: Taurus, Polaris

1. LARGE SCALE RESULTS ON DIFFUSE CLOUDS

The correlation study between the DIRBE and FIRAS data and HI emission from the Dwingeloo survey has shown that, on average, dust associated to neutral Hydrogen in high latitude cirrus clouds reaches an equilibrium temperature of 17.5 K (assuming a dust emissivity index of 2 in the sub-millimeter) in the solar neighborhood (Boulanger et al. 1996). The high latitude dust also exhibits, on average, an emissivity value very close from that predicted by the model of Draine and Lee 1984. Similarly, the FIRAS/WHAM correlation has allowed the first characterization of dust associated to the diffuse ionized gas Lagache et al. 2000, showing similar properties as the ones for HI associated dust. However, these studies could only derive average values over a large fraction of the sky at high latitude and the homogeneity of the dust temperature and/or emission properties cannot be tested on smaller scales, due

to the limited sensitivity of the FIRAS data. At higher angular resolution, the IRAS data has shown the existence of a wide variety of IR color changes in the ISM. These include I_{12}/I_{100} color variations (e.g. Boulanger et al. 1990) which are observed toward HII regions where they are interpreted as PAH destruction in regions with high radiation field, as well as toward haloes surrounding some translucent clouds (e.g. Bernard et al. 1992) where they reflect PAH overabundances, possibly linked to PAH desorption from the surface of larger grains. Extreme cases have recently been evidenced using the ISO data, where PAH abundance have been demonstrated to vary by large factors (as high as 10) within a diffuse cirrus cloud in Ursa Major (Miville-Deschênes 2000). In this case, the comparison between the ISO and interferometer HI data obtained using the Dominion Radio Astrophysical Observatory (DRAO) shows a strong correlation with the HI line-width, indicating for the first time a possible connection of the abundance of the smallest dust particles with turbulence.

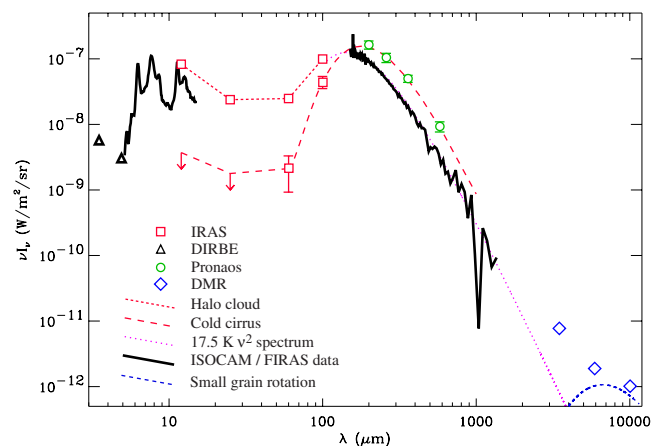


Figure 1. Average diffuse ISM spectrum. The ISOCAM and FIRAS spectra are shown as black curves and the DIRBE broad band measurements as triangles. The range of known variations in observed SEDs is illustrated by the spectrum of cold dust from a cirrus cloud in Polaris and of a bright mid-IR halo cloud in Chamaeleon. The DMR data showing evidence for small grain rotation is shown as diamonds. All data has been scaled to $N_H = 4 \times 10^{20} \text{ H/cm}^2$ ($A_V = 0.2$).

Similarly, regions with low $60\ \mu\text{m}$ relative to their $100\ \mu\text{m}$ emission have been evidenced (Laureijs et al. 1991, Abergel et al. 1994) in difference maps between the two IRAS bands. They seem to closely correspond to molecular regions (as in the Taurus molecular complex), but not all molecular clouds show the trend (e.g. the ρ -Ophiuchi molecular cloud). Under recent dust models which include transient heating of small dust particles (Désert et al. 1990), these variations are readily interpreted as a lack of intermediate size particles (VSGs, Very Small Grains). Originally, these regions were referred to as "cold clouds" owing to their distinctive IRAS colors. However, since different dust particles (VSGs and BGs respectively) dominate the IR emission at 60 and $100\ \mu\text{m}$, the temperature derived from the I_{60}/I_{100} ratio is not physical. Large scale measurements with DIRBE showed that, on average, dust toward these regions was indeed colder than the average ISM (Lagache et al. 1988), but no clear physical interpretation could be given. Measuring the actual temperature of large grains on small scale toward these regions has become possible only recently with ISO and balloon-borne measurements (see next section).

Therefore, large abundance variations of small dust particles (PAH and VSG) seems fairly common in the ISM, although the origin of these variations is not yet understood. This is illustrated in Fig. 1 which shows the average dust emission at high latitude and extreme Spectral Energy Distributions observed toward VSG deficient and PAH overabundant regions.

In the millimeter range, a combined analysis of the FIRAS and DMR data toward diffuse regions shows evidence for excess emission relative to that of dust associated with HI gas (e.g. Kogut et al. 1996). As shown by Draine and Lazarian 1999, this excess in the longest wavelength DMR channels can be accounted for by free-free emission and emission from rotating small dust particles. It is therefore expected that dust emission above a few millimeters will be dominated by small dust particles. Note that the extrapolation of the $T = 17.5\ \text{K}\ \nu^2$ spectrum does not explain the DMR measurement at $3.3\ \text{mm}$, leaving room for yet another dust component such as very cold dust.

2. THE PRONAOS EXPERIMENT

The balloon-borne experiment PRONAOS¹ ("PROjet National d'Observation Submillétrique") consist of a gondola hosting a 2m segmented submillimeter telescope. The observations presented here were taken during the second flight from Fort-Sumner (NM, USA) on September 22 1996 during which data could be obtained under good conditions for more than 20 hours. The fine pointing of the payload is ensured by a star tracker allowing night and

¹ PRONAOS was built as a national cooperation involving the *Centre National de Recherche Scientifique* (CNRS) and the *Centre National d'Etudes Spatiales* (CNES).

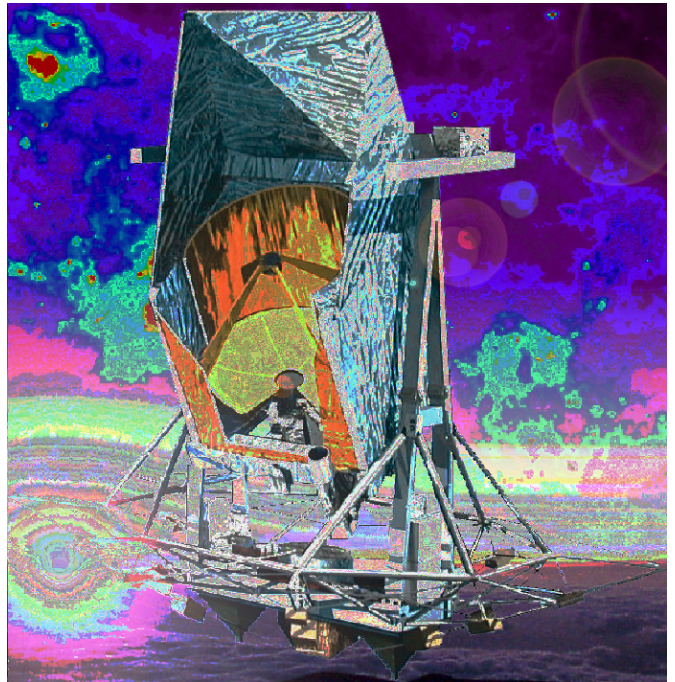


Figure 2. Schematics of the PRONAOS Gondola. Several sub-systems can be identified (from top to bottom): Telescope shutter, secondary mirror, segmented primary mirror, SPM focal plane instrument (in the back), stellar sensor, landing structure (reverse umbrella shaped tubular structure) and ballast hoppers. The overall height of the gondola is 8 m. Its total weight is 2 tons.

day detection of stars to a relative accuracy of about 5" rms.

The focal plane instrument, SPM ("Spectro Photomètre Submillétrique"), is a submillimeter photometer observing simultaneously in four channels at 200 , 260 , 360 and $580\ \mu\text{m}$ (effective wavelengths for a ν^2 emissivity grey body spectrum at $30\ \text{K}$) in wide bands ($\Delta\lambda = 60$, 100 , 200 and $560\ \mu\text{m}$ respectively). A detailed description of the SPM photometer and the PRONAOS gondola and telescope is given in Lamarre et al. 1994. The beam of the instrument is modulated on the sky with an amplitude of $6.0'$ at a frequency of $20\ \text{Hz}$ using an internal wobbling mirror. Detection is achieved using four bolometers cooled to $0.3\ \text{K}$ by two compact, closed cycle ^3He fridges. The FWHM beam size, as measured on a map of Saturn during the flight, is $2'$, $2'$, $2.5'$ and $3.5'$ respectively. The in-flight response of the SPM instrument is measured using a dual temperature internal calibration system. Variations of the response are lower than 10% in all 4 bands and the relative uncertainty between photometric bands is less than 5%.

In all cases, the PRONAOS maps were smoothed to the resolution of the long wavelength channel ($3.5'$) and the data was combined to the IRAS measurements at 60 and $100\ \mu\text{m}$, in order to extend the available spectral information. Since the PRONAOS data are obtained using

beam modulation on the sky which subtracts out low spatial frequencies, an accurate comparison requires a similar subtraction in the IRAS data. This is accomplished by simulating the PRONAOS observing strategy (modulation, scanning, beam size) on the IRAS ISSA maps. From then on, the same data reduction as for the PRONAOS data (deconvolution, averaging, ...) is applied to the simulated IRAS data.

3. PRONAOS OBSERVATIONS OF TRANSLUCENT CLOUDS

Two diffuse clouds were observed using PRONAOS during the 1996 flight, in the Polaris flare (MCLD 123.5 + 24.9; Bernard et al. 1999) and the Taurus region (Stepnik et al. 2001). Visual extinction maps toward those clouds were obtained through star counts in the PMM-USNO catalog in the B band, following the procedure described in Cambr y 1999. The extinction measured toward the two clouds is low ($A_v = 0.8$ mag for MCLD 123.5+24.9) to intermediate ($A_v = 3.9$ mag for the Taurus filament). Both clouds have well detected molecular emission, and exhibit a large $I_{100} - I_{60}$ IRAS excess indicating a strong VSG abundance deficiency.

A detailed analysis of of the Pronaos Taurus data is given in Stepnik et al. in these proceedings. Toward the inner regions of the filaments, the best χ^2 fit to the SPM and IRAS data at $100 \mu\text{m}$, taking into account the uncertainties on each measurement (errors quoted at the 68% confidence level), leads to a dust temperature and a sub-millimeter emissivity index of $T_d = 12.3 \pm 0.4 \text{ K}$ and $\beta = 1.9 \pm 0.2$ respectively. The emission from the outer regions of the cloud was also detected by PRONAOS and shows higher dust temperature values ($T_d = 14.8 \pm 0.6 \text{ K}$) than toward the center. The transition between the extended envelope and the cold filament core is not resolved by the PRONAOS observations (i.e. is smaller than $3.5'$) but corresponds precisely to the region where the $I_{100} - I_{60}$ IRAS excess changes abruptly, strongly pointing toward a physical connection between the two effects. Similarly cold dust and steep emissivity index ($T_d = 13.0 \pm 0.8 \text{ K}$ and $\beta = 2.2 \pm 0.3$) have been evidenced toward the cirrus MCLD 123.5 + 24.9.

For both clouds, it could be demonstrated that the low dust temperatures observed cannot be explained by the radiative transfer of UV photons from the Interstellar Radiation Field (ISRF) through the cloud. Instead, it is necessary to invoke a change in the optical properties of the emitting grains in the abnormally cold regions of the clouds. Since the cold regions also present strong VSG deficiency, we proposed (Bernard et al. 1999) that the change of the BG optical properties may be due to the coagulation of VSGs with larger grains. Fractal grains generally have increased emissivity in the FIR (e.g. Wright 1987, Bazell and Dwek 1990) which tends to lower their equilibrium temperature. Dust coagulation could therefore provide a natural explanation both to the reduced

abundance of VSG and to the low dust temperature observed. A more quantitative study of the submillimeter emission of the Taurus filament was performed by Stepnik et al. 2001, which included radiative transfer within a cylindrical geometry and incorporated realistic optical properties for fractal grains. They showed that the submillimeter emission profiles across the Taurus filament are consistent with the standard dust distribution proposed by D sert et al. 1990 in the outskirts of the cloud, but requires an abrupt change of the properties in the inner regions ($n_H > 3 \cdot 10^3 \text{ H/cm}^3$, $A_v > 2.0$). The required increase of the submillimeter emissivity is of the order of 3.4 times that of standard large grains. In the framework of fractal grains composed of individual standard large grains, this can be achieved with very porous (volume filling factors of a few %) fluffy aggregates containing up to 200 individual grains. This is expected to be an upper limit since the Q_{abs} calculation did not incorporate the presence of graphite dominated VSG in the aggregate and the submillimeter emissivity enhancement of graphite aggregates is known to be $\simeq 6$ times more efficient than for silicate ones (Stognienko et al. 1995).

4. PRONAOS OBSERVATIONS OF STAR FORMING REGIONS

Several nearby star forming regions have been observed with PRONAOS, including the Orion nebula (Ristorcelli et al. 1998, Dupac et al. 2001), ρ -Ophiuchi and M17. The observations toward the Orion Nebula have allowed to detect low brightness clouds away from the very bright areas corresponding to regions currently forming stars. These clouds exhibit low dust temperatures, down to $T_d=12\text{K}$. Their origin is still not understood and their low submm brightness makes additional ground observations very difficult.

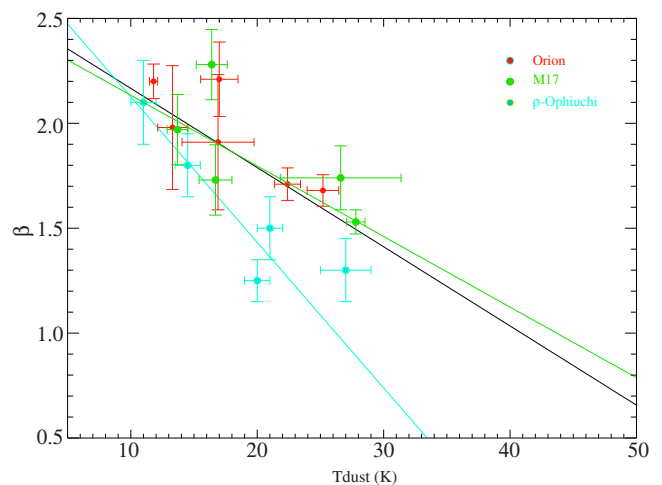


Figure 3. Anti-correlation between dust equilibrium temperature and emissivity index as observed using PRONAOS toward several nearby star forming regions.

Figure 3 shows the emissivity index plotted against dust temperature for several dust condensations observed in the above star forming regions. A clear anti-correlation (correlation coefficient of the order of -0.9) is observed between these two parameters for the 3 regions. Note that the fitting procedure used to derive T_d and β induces a natural anti-correlation between these two parameters. However, the resulting correlation coefficient for a population of spectra with no intrinsic parameter correlation was found to be -0.4, well below the observed value (Dupac et al. 2001). The observed anti-correlation therefore reflects actual changes of the submillimeter optical dust properties with temperature. Interestingly, a similar trend has been observed in the few laboratory studies which could measure optical properties of bulk silicates at low temperature (Agladze et al. 1996, Menella et al. 1998). They may reflect quantum processes within the grains appearing only at low temperature. To our knowledge, this is the first time such effects are evidenced in the ISM.

5. IMPLICATIONS FOR FIRST SURVEYS

Recent sensitive observations in the IR and sub-millimeter have evidenced unexpected dust properties such as low equilibrium temperatures toward some cirrus or translucent clouds and the existence of a significant anti-correlation between the dust temperature and emissivity index in nearby star forming regions. However, the available balloon data are still very incomplete and possibly very much biased toward extreme regions, while the poor angular resolution of existing satellite data generally prevents detailed studies of individual regions and precise physical interpretation. In the millimeter range, dust emission is likely dominated by the rotation of very small dust particles, which abundance in the diffuse ISM is known to vary with physical conditions such as density or turbulence and to be affected by shocks. Therefore, the dust emission in the FIR-mm wavelength range may be far more complex than previously anticipated. This has direct implications upon future cosmology missions (such as Planck) which will require precise subtraction of Galactic foregrounds in the millimeter.

Large surveys which can be undertaken with FIRST within dedicated key programs will offer the possibility to understand the physical processes which are responsible for the variations of the dust size distribution and optical properties in the diffuse ISM with unprecedented angular resolution. Combining these data with the all-sky Planck survey will allow to characterize the dust emission properties over the whole FIR-mm wavelength range. Surveys for Young Stellar Object that will be undertaken with FIRST toward molecular clouds should also be well suited to constrain dust properties in opaque regions of the ISM (say $A_v > 10$). Dust properties in very diffuse parts of the ISM (say $A_v < 0.1$), which are of particular importance for understanding foreground contamination

in the Planck data, should also emerge from the currently planned FIRST shallow cosmological surveys. However, we have seen that several important transitions affecting dust properties are taking place at intermediate column densities. This strongly calls for a large scale survey with PACS and SPIRE targeting at dust emission from intermediate column density regions ($0.1 < A_v < 10$) of the ISM.

In the mean time, the next step in our steady understanding of the FIR-mm emission properties of interstellar dust is expected to come from the all sky survey of the Japanese astro-F mission at $160\mu\text{m}$ as well as from the ELISA balloon-borne experiment (see Ristorcelli et al. in these proceedings) which will map a large fraction of the sky in the wavelength range relevant to FIRST, and will be available for planning future large scale surveys with FIRST.

REFERENCES

- Abergel A., Boulanger F., Mizuno A. et al., 1994, ApJ 423, 59.
 Agladze N.I, Sievers A.J., Jones S.A. et al. 1996, ApJ 462, 1026
 Bazell D. & Dwek E., 1990, ApJ 360, 142.
 Bernard J.-P., Boulanger F., Désert F.X. et al., 1992, A&A, 263, 258.
 Bernard J.-P., Abergel A., Ristorcelli I. et al., 1999, A&A, 347, 640.
 Boulanger F., Falgarone E., Pujet J.-L. et al. 1990, ApJ 364, 136.
 Boulanger F., Abergel A., Bernard J.-P. et al., 1996, A&A 312, 256.
 Cambrésy L., 1999, A&A 345, 965.
 Désert F.-X., Boulanger F., Pujet J.-L. 1990, A&A 237, 215.
 Draine B.T. & Lee H.M., 1984, ApJ 285, 89.
 Draine B.T. & Lazarian A., 1999, ApJ 512, 740.
 Dupac X., Giard M., Bernard J.P. et al. 2001, accepted in ApJ.
 Kogut A., Banday A.J., Bennett C.L. et al. 1996, ApJ 460, 1.
 Lagache G., Abergel A., Boulanger F., Pujet J.-L. 1998, A&A 333, 709.
 Lagache G., Haffner L.M., Reynolds R.J. et al. 2000, A&A 354, 247.
 Lamarre J.-M., Pajot F., Torre J.-P. et al., 1994, IR Phys. Techno., 35, 277.
 Laureijs R. J., Clark F. O., Prusti T. 1991, ApJ 371, 602.
 Menella V., Brucato J. R., Colangeli L. et al. 1998, ApJ 496, 1058.
 Mivilles-Deschênes M.A. 2000, PhD thesis.
 Ristorcelli I., Serra G., Lamarre J.M. et al 1998, A&A 496, 267.
 Stepnik B. et al 2001 submitted to A&A.
 Stognienko R., Henning T., Ossenkopf V. 1995, A&A 296, 797.
 Wright E.L., 1987, ApJ 320,818.